European Journal of Medicinal Chemistry 46 (2011) 588–599

Contents lists available at ScienceDirect

European Journal of Medicinal Chemistry

journal homepage: http://www.elsevier.com/locate/ejmech

Original article

Characterization of the baicalein–bovine serum albumin complex without or with Cu^{2+}or Fe^{3+} by spectroscopic approaches

Daojin Li, Mei Zhu, Chen Xu, Baoming Ji*

College of Chemistry and Chemical Engineering, Luoyang Normal University, Longmen Road 71#, Luoyang 471022, China

ARTICLE INFO

Article history:
Received 16 August 2010
Received in revised form
27 October 2010
Accepted 23 November 2010
Available online 1 December 2010

Keywords:
Baicalein
Bovine serum albumin
Fluorescence quenching
Circular dichroism
Three-dimensional fluorescence

ABSTRACT

The binding of baicalein to bovine serum albumin (BSA) in the absence and presence of Cu^{2+} or Fe^{3+} in aqueous solution has been studied by fluorescence, synchronous fluorescence, ultraviolet–visible (UV–vis) spectra, circular dichroism (CD) and the three-dimensional (3D) fluorescence at pH 7.40. The decrease of the binding constant in the presence of Cu^{2+} or Fe^{3+} may result from the competition of the metal ions and baicalein binding to BSA. The effect of baicalein on the conformation of BSA was analyzed using UV, CD, fluorescence and three-dimensional (3D) fluorescence. These results indicate that the binding of baicalein to BSA causes apparent change in the secondary structure of BSA, but does not affect the polarity around the chromophore molecule.

1. Introduction

The interaction between bio-macromolecules and drugs has attracted great interest among researchers since several decades [1–3]. Over the past years, much research has been focused on two central questions about proteins: what are the determinant factors that influence on the protein structures and functions, and how does a factor affect their biological activity [4–8]. Serum albumin (SA), the main protein in the blood plasma acting as the transporter and disposition of many drugs, has been frequently used as a model protein for investigating the protein folding and ligand-binding mechanism. In this regard, bovine serum albumin (BSA) has been studied extensively, partly because of its structural homology with human serum albumin (HSA) [9–13]. BSA (Scheme 1) is composed of three linearly arranged, structurally homologous sub-domains (A, B). It has two tryptophan residues that possess intrinsic domains (I–III) and each domain in turn is the product of two fluorescence: Trp-134, which is located on the surface of sub-domain IB, and Trp-212, locating within the hydrophobic binding pocket of sub-domain IIA [14]. The binding sites of BSA for endogenous and exogenous ligands may be in these domains and the principal regions of drugs binding sites of albumin are often located in hydrophobic cavities in sub-domains IIA and IIIA. So called sites I and II are located in sub-domain IIA and IIIA of albumin, respectively.

Baicalein (Scheme 2), the major flavonoid derived from the root of *Scutellaria baicalensis*, has been commonly used in traditional Chinese medicine for inflammation, suppurative dermatitis, respiratory tract infection, diarrhea, jaundice, hepatitis, allergic disease and cancer [15,16].

The binding study of drugs with proteins is of great importance in pharmacy, pharmacology and biochemistry. There are also some metal ions present in blood plasma, which can affect the binding of the drugs and serum albumins. They could participate in many biochemical processes. Some plasma proteins (serum albumin) usually act as sequestration agent of metal ions and have a variety of metal sites with different specificities and the phenomenon of serum albumin molecular conformational alteration caused by metal ions–BSA (or HSA) binding could be observed in some metal ions–BSA (or HSA) interaction process. Furthermore, many metal ions could form complex with medicine molecules, and affect some characters of drug. So it is reasonable to ratiocinate that metal ions would affect the interaction of medicine molecules with BSA (or HSA) in a ternary system of drug–protein–metal ion, and thus it would influence the distribution, pharmacological property, and metabolism of medicine in blood. In addition, Cu^{2+} or Fe^{3+} is an essential life element in the human body and plays important structural and functional roles in many proteins. Therefore, it is necessary to investigate the interaction of BSA–baicalein in the presence of metal ions, especially Cu^{2+} or Fe^{3+}.

* Corresponding author. Tel.: +86 379 65523821.
E-mail address: lyhxxjbm@126.com (B. Ji).

0223-5234/$ – see front matter © 2010 Published by Elsevier Masson SAS.
doi:10.1016/j.ejmech.2010.11.038

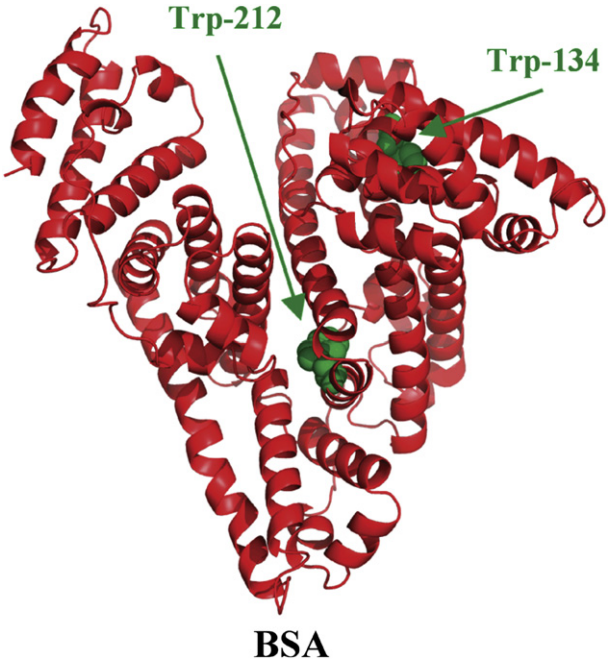

Scheme 1. Structure of BSA, with tryptophan residues shown in green color (For interpretation of the references to color in this figure legend, the reader is referred to the web version of this article.).

The interaction between BSA (or HSA) and a few kinds of medicine, such as daunorubicin [17], carnitine [18] in the presence of Cu^{2+} or Fe^{3+} has been reported. However, there is no report about the influence of Cu^{2+} or Fe^{3+} on the interaction between baicalein and BSA. To explore the influence of Cu^{2+} or Fe^{3+} on the interaction between baicalein and BSA, in this study, we have investigated the interaction between baicalein and BSA without or with Cu^{2+}or Fe^{3+} by means of fluorescence spectra, three-dimensional (3D) fluorescence spectra, UV spectra, CD spectra.

2. Results and discussion

2.1. Fluorescence quenching studies of BSA by baicalein in the absence and presence of Cu^{2+} or Fe^{3+}

The fluorescence spectra of BSA with baicalein in the absence and presence of Cu^{2+} or Fe^{3+} were measured with an excitation wavelength of 295 nm (Fig. 1). As we see, BSA exhibits a strong fluorescence emission band at 344 nm. Its intensity decreased gradually with the addition of baicalein regardless without or with Cu^{2+} and Fe^{3+}, i.e., the excited BSA was quenched by baicalein regardless of metal ions. The emission peak position and shape with Cu^{2+} or Fe^{3+} at different concentrations of baicalein were similar to that without Cu^{2+} or Fe^{3+}, while the emission intensity of BSA in the presence of Cu^{2+} or Fe^{3+} was a little weaker than that in the absence of Cu^{2+} or Fe^{3+}.

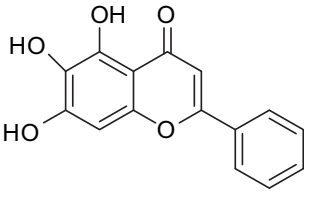

Scheme 2. Chemical structure of baicalein.

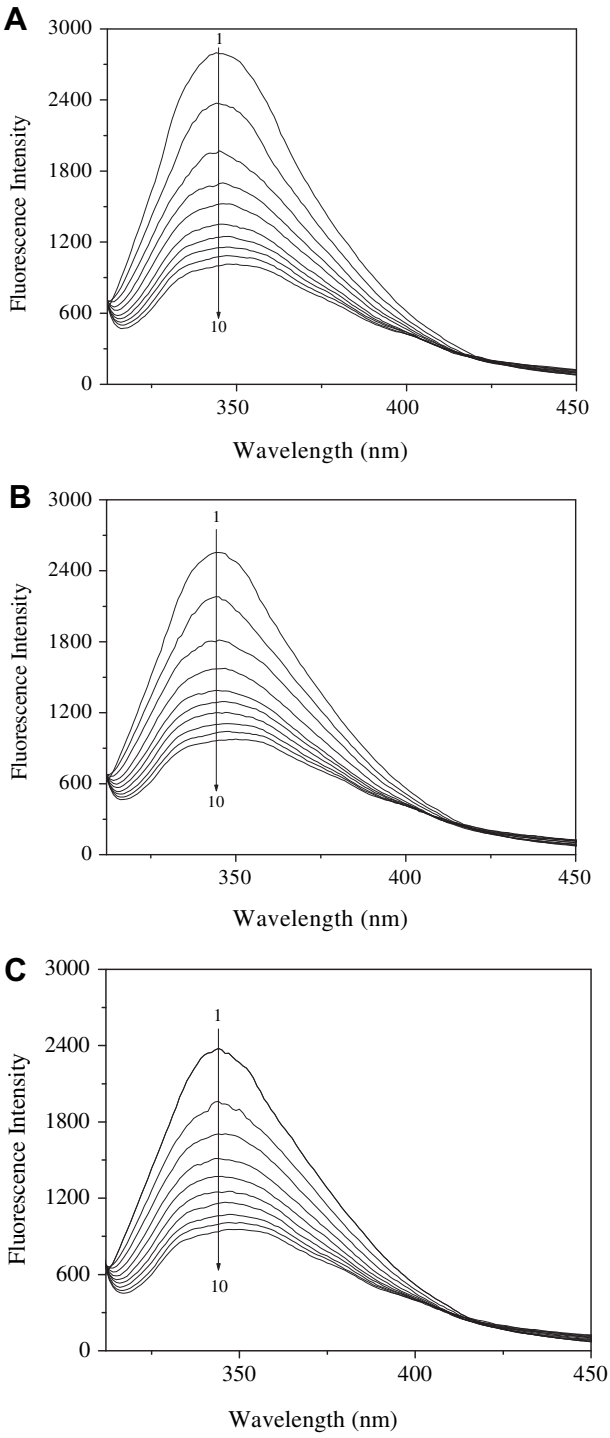

Fig. 1. Fluorescence spectra of baicalein–BSA systems without Cu^{2+} or Fe^{3+} (A) and with Cu^{2+} (B), Fe^{3+} (C). (1–10) The concentrations of baicalein are (μM): 0, 1, 2, 3, 4, 5, 6, 7, 8 and 9. [BSA] = 4.5 μM.

This result implies that the fluorescence quenching mechanism, in the absence and presence of Cu^{2+} or Fe^{3+} involved, may be rationalized in terms of a static quenching process.

2.2. Quenching mechanism analysis

To elucidate further the quenching mechanism of BSA induced by baicalein, the fluorescence quenching data are analyzed with the Stern–Volmer equation (Eq. (1)) [19]:

$$\frac{F_0}{F} = 1 + k_q\tau_0[Q] = 1 + K_{SV}[Q] \quad (1)$$

where F_0 and F are the relative fluorescence intensities in the absence and presence of quencher, respectively, [Q] is the concentration of quencher, K_{SV} the Stern–Volmer dynamic quenching constant, k_q the bimolecular quenching rate constant, τ_0 the average bimolecular lifetime in the absence of quencher evaluated at about 5 ns [20–22]. Fig. 2 shows the plot of F_0/F for BSA versus [Q] of baicalein in the absence and presence of Cu^{2+} or Fe^{3+} ranging from 1 to 9 μM of baicalein at 310 K. Linear fittings (in Fig. 2) of the experimental data obtained afford K_{SV} and k_q (Table 1). For dynamic quenching, the maximum scattering collision quenching constant of various quenchers is 2.0×10^{10} L mol^{-1} s^{-1} [23]. The results showed that the value of k_q was much greater than 2.0×10^{10} L mol^{-1} s^{-1}, which indicated that the probable quenching mechanism of fluorescence of BSA by baicalein without or with Cu^{2+} or Fe^{3+} is not caused by dynamic collision but from the formation of a complex.

This recognition can be also confirmed by the analysis of Stern–Volmer plot at different concentrations of BSA. It is well-known that the Stern–Volmer equation is fit for both dynamic and static quenching mechanism. Nevertheless, the Stern–Volmer slope (K_{SV}) is expected to depend on the concentration of BSA in a static quenching process, whereas the slope does not change at any concentration of BSA in only a dynamic process. Fig. 3 shows plots of F_0/F versus [Q] at different concentrations of BSA at pH 7.40 and the values of K_{SV} were presented in Table 2. Obviously, it can be seen that the values for slopes decrease with increasing concentrations of BSA. It again indicated that the quenching arises from the complex formation rather than a dynamic process.

2.3. Influences of common ions (Cu^{2+} or Fe^{3+}) on binding constant

Metal ions are vital to human body and playing an essentially structural role on many proteins based on coordinate bonds. The presence of metal ions in body may affect interaction of drugs with BSA. Effects of common metal ions (e.g. Cu^{2+} and Fe^{3+}) on binding constants of baicalein–BSA complex were investigated at 310 K.

When small molecules bind independently to a set of equivalent sites on a macromolecule, the equilibrium between free and bound molecules is given by the following equation [24]:

Table 1
Stern–Volmer quenching constants of the system of baicalein–BSA with or without Cu^{2+}, Fe^{3+}. R is the correlation coefficient, $C_{BSA} = C_{Cu^{2+}} = C_{Fe^{3+}} = 4.5 \times 10^{-6}$ M.

pH	T (K)		K_{SV} ($\times 10^5$ L/mol)	k_q ($\times 10^{13}$ L mol^{-1} s^{-1})	R
7.40	310	Baicalein–BSA	1.96	3.92	0.9979
		Baicalein–BSA–Cu^{2+}	1.76	3.52	0.9964
		Baicalein–BSA–Fe^{3+}	1.60	3.20	0.9992

$$\log\frac{(F_0 - F)}{F} = \log K + n\log[Q] \quad (2)$$

where K and n are the binding constant and the number of binding sites, respectively.

Plots of log $(F_0 - F)/F$ versus log [Q] for baicalein–BSA in the absence and presence of Cu^{2+} or Fe^{3+} are shown in Fig. 4. The values of binding constant K and the number of binding sites per BSA acquired in the absence and presence of metal ions are listed in Table 3. It can be inferred from the values of n that there is about one independent class of binding sites on BSA in the absence and presence of Cu^{2+} or Fe^{3+} for the ligand. The results also illustrated that there is a modest strong binding force between baicalein and BSA. He and Carter have reported that serum albumin has a limited number of binding sites for endogenous and exogenous ligands that are typically bound reversibly and have binding constants 10^4–10^8 [7,25]. The sufficient K value to make an interaction between ligand and protein would be larger than 10^4.

It also can be observed from Table 3 that the presence of Cu^{2+} or Fe^{3+} ions decreased the binding constants and binding sites of baicalein–BSA complex, indicating that Cu^{2+} or Fe^{3+} would affect the binding capacity of baicalein binding to BSA. Thus, the decrease in binding constant of baicalein–BSA in presence of the above ions shortens storage period of baicalein in blood plasma and enhances its maximum effects. The smaller binding constants possibly result from two aspects as follows: there is the existence of the competition of metal ions and baicalein binding to BSA, which may decrease the binding capability of baicalein to BSA; or Cu^{2+} or Fe^{3+} induced the conformational changes of BSA, which is more difficult for baicalein binding to BSA.

In order to further confirm the binding feature of Cu^{2+} or Fe^{3+} in baicalein–BSA system, the binding distances (r) between the

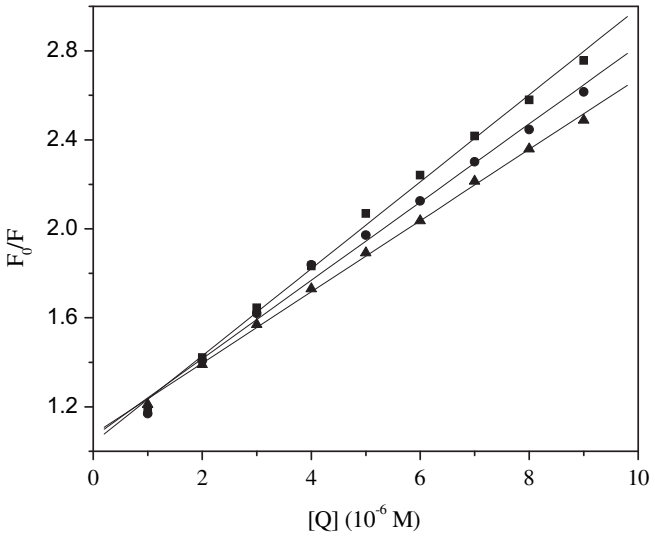

Fig. 2. Stern–Volmer plot of the fluorescence quenching of BSA with different concentrations of baicalein: ■ baicalein–BSA systems; ● baicalein–BSA–Cu^{2+} systems; ▲ baicalein–BSA–Fe^{3+}.

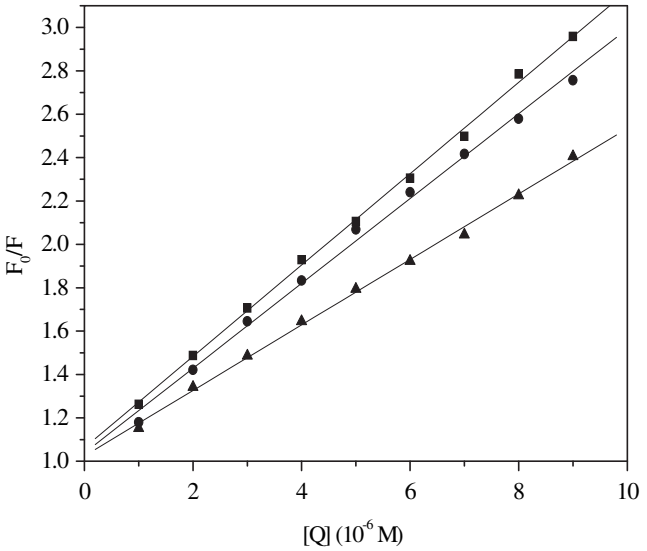

Fig. 3. Stern–Volmer plots for the baicalein–BSA system at different concentrations of BSA at 310 K with pH = 7.40: ■ [BSA] = 3 μM; ● [BSA] = 4.5 μM; ▲ [BSA] = 6 μM.

Table 2
Stern–Volmer quenching constants for the baicalein–BSA system at pH 7.4, *R* is the correlation coefficient.

T (K)	[BSA]($\times 10^{-6}$ L mol^{-1})	K_{SV} ($\times 10^{5}$ L mol^{-1})	k_q ($\times 10^{13}$ L mol^{-1} s^{-1})	*R*
310	3.0	2.11	4.22	0.9992
	4.5	1.96	3.92	0.9979
	6.0	1.51	3.02	0.9988

acceptor (baicalein) and the donor (BSA) were determined by Förster's theory of dipole–dipole energy transfer [26,27], in which the spatial orientation factor of the dipole $k^2 = 2/3$, the refractive index of medium $N = 1.36$ and the fluorescence quantum yield of donor $\Phi = 0.14$ are obtained [28,29]. *J* can be evaluated by integrating the overlap (Fig. 5) of the absorption spectrum of baicalein with the fluorescence emission spectrum of BSA in the absence and presence of Cu^{2+} or Fe^{3+}. Fluorescence resonance energy transfer (FRET) is a nondestructive spectroscopic method that can monitor the proximity and relative angular orientation of fluorophores, the donor and acceptor fluorophores can be entirely separate or attached to the same macromolecule. A transfer of energy could take place through direct electrodynamic interaction between the primarily excited molecule and its neighbors, with an important condition: the distance between the donor and the acceptor is approach in the range of 2–8 nm (Weiss, 1999). All the results are shown in Table 4. The distance of donor to acceptor, $r < 8$ nm, indicates the non-radiative energy transfer coming into being between baicalein and BSA with or without Cu^{2+} or Fe^{3+} [30].

Comparing *r* in the absence of Cu^{2+} or Fe^{3+} with that in the presence of Cu^{2+} or Fe^{3+}, the small changes of *r* could be explained by the possibility of the existence of the competition of metal ions and baicalein binding to BSA rather than the conformational changes of BSA induced by Cu^{2+} or Fe^{3+}. This result also can be supported by CD mentioned below.

2.4. The binding mode

Intermolecular interacting forces between a small molecule and a biomacromolecule include hydrogen bond, van der Waals force, electrostatic and hydrophobic interactions, etc. Thermodynamic parameters for a binding interaction can be used as a major evidence

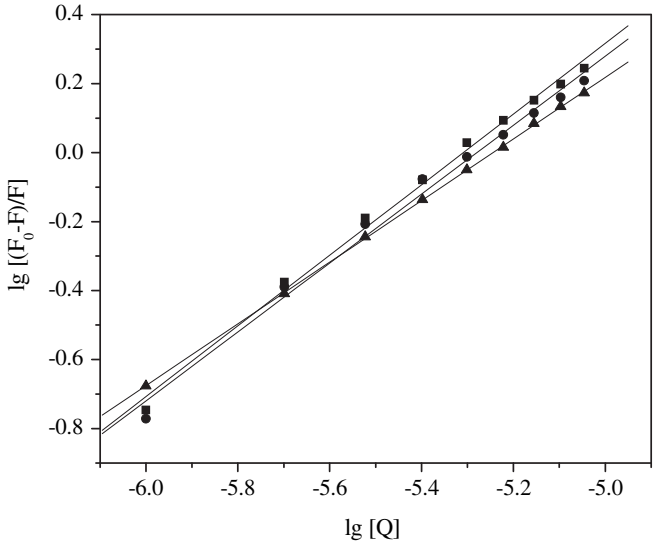

Fig. 4. Logarithmic plot of the fluorescence quenching of BSA with different concentrations of baicalein: ■ baicalein–BSA systems; ● baicalein–BSA–Cu^{2+} systems; ▲ baicalein–BSA–Fe^{3+} systems.

Table 3
Binding parameters for baicalein–BSA interaction in the absence and presence Cu^{2+} or Fe^{3+} at pH 7.4. *R* is the correlation coefficient, $C_{BSA} = C_{Cu^{2+}} = C_{Fe^{3+}} = 4.5 \times 10^{-6}$ M.

	K (L mol^{-1})	*n*	*R*
Baicalein–BSA	2.70×10^5	1.02	0.9973
Baicalein–BSA–Cu^{2+}	1.88×10^5	1.00	0.9950
Baicalein–BSA–Fe^{3+}	4.85×10^4	0.90	0.9999

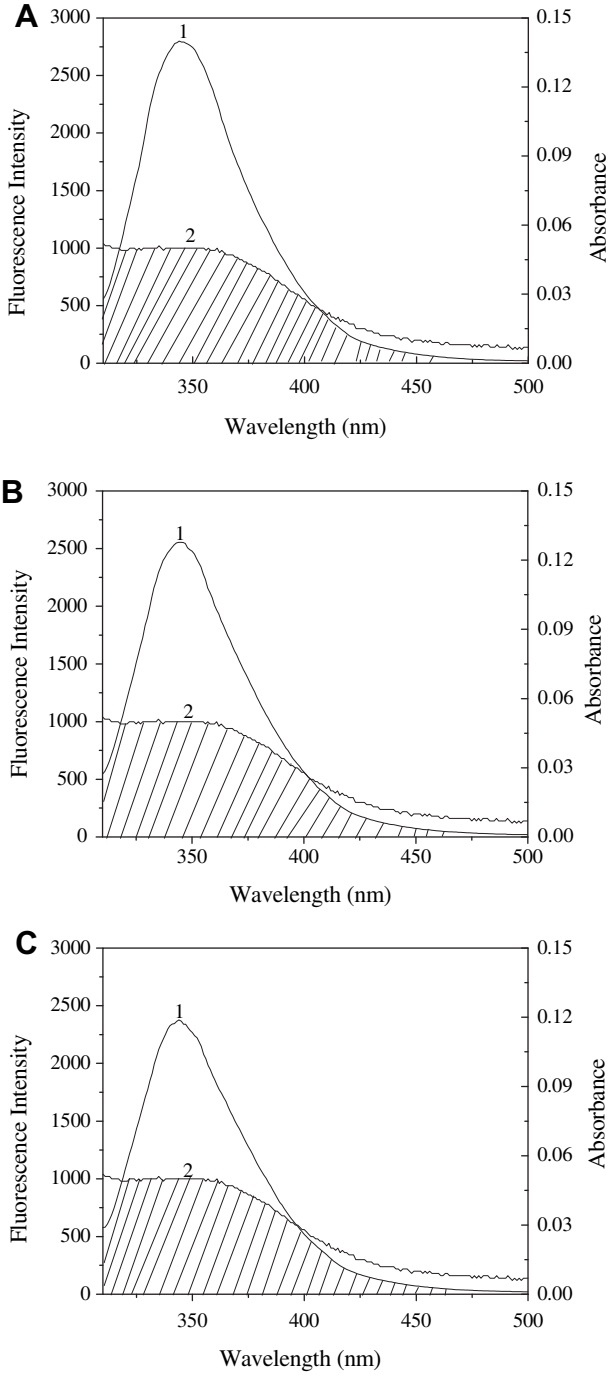

Fig. 5. Overlap between the fluorescence emission spectrum of BSA (1) and UV absorption spectrum of baicalein (2). (A) baicalein–BSA system: 4.5 μM baicalein + 4.5 μM BSA; (B) baicalein–BSA–Cu^{2+} system: 4.5 μM baicalein + 4.5 μM BSA + 4.5 μM Cu^{2+}; (C) baicalein–BSA–Fe^{3+} system: 4.5 μM baicalein + 4.5 μM BSA + 4.5 μM Fe^{3+}.

Table 4
The calculated J, E and r values of baicalein–BSA in the presence and absence of Cu^{2+} or Fe^{3+}.

	J (cm^3 L mol^{-1})	E (%)	R_0 (nm)	r (nm)
Baicalein–BSA	2.36×10^{-15}	48.1	2.41	2.44
Baicalein–BSA–Cu^{2+}	2.28×10^{-15}	46.4	2.39	2.45
Baicalein–BSA–Fe^{3+}	2.22×10^{-15}	48.0	2.38	2.42

to learn the binding mode. Thus, the temperature-dependent thermodynamic parameters for the baicalein–BSA system are used to characterize the intermolecular forces between baicalein and BSA. The enthalpy change ΔH^0 and entropy change ΔS^0 for a binding reaction can be derived from the van't Hoff equations (Eq. (3)):

$$\ln K = -\Delta H^0/RT + \Delta S^0/R \quad (3)$$

where K is the binding constant at the corresponding temperature and R the gas constant. The binding constants of baicalein to BSA were calculated to be 4.78×10^5 L mol^{-1}, 3.82×10^5 L mol^{-1}, 2.70×10^5 L mol^{-1}at 290 K, 300 K and 310 K, respectively. The enthalpy change ΔH^0 and entropy change ΔS^0 were obtained from the slope and intercept of the linear van't Hoff plot (Fig. 6) of ln K versus $1/T$ based on Eq. (3). The values of ΔH^0 and ΔS^0 for baicalein binding to BSA are evaluated to be -20.4 kJ mol^{-1} and 38.3 J mol^{-1} K^{-1}, respectively. From the point of view of water structure, for a drug–protein interaction, a positive ΔS^0 value is frequently regarded as an evidence for a hydrophobic interaction [31] because the water molecules that are arranged in an orderly fashion around the drug and protein acquire a more random configuration. Furthermore, the negative ΔH^0 value (-20.4 kJ mol^{-1}) observed cannot be mainly attributed to electrostatic interactions since for electrostatic interactions ΔH^0 is very small, almost zero [32,33]. A negative ΔH^0 value indicates that there is hydrogen bond in the binding process. Therefore, it is not possible to account for the thermodynamic parameters on the basis of a single intermolecular force model. So, hydrophobic forces most likely play a major role in the binding of baicalein to BSA, but hydrogen bonding also cannot be excluded. The study would be helpful for new drug design.

2.5. Conformation investigation of BSA induced by baicalein in the absence and presence of metal ions

2.5.1. UV–vis absorption studies

UV–vis absorption measurement is a very simple method and applicable to explore the structural change and to know the complex formation [34]. UV–vis absorption spectra of BSA with various amounts of baicalein without and with Cu^{2+} or Fe^{3+} (Fig. 7) were obtained by subtracting corresponding to the spectrum of baicalein-free form in the buffer from that of baicalein–BSA complex. It can be observed that the UV–vis absorption spectrum of BSA shows a strong band with a maximum at 208 nm and a weak band with a maximum at 279 nm. The absorbance (208 nm) intensity of

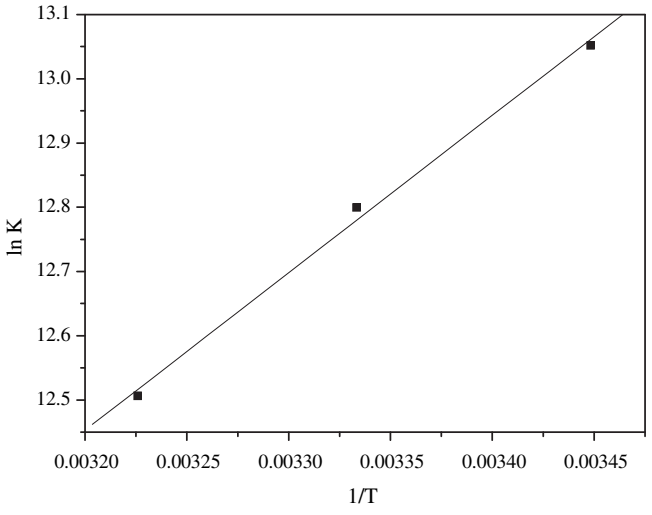

Fig. 6. van't Hoff plot for the interaction of BSA with baicalein at pH 7.40.

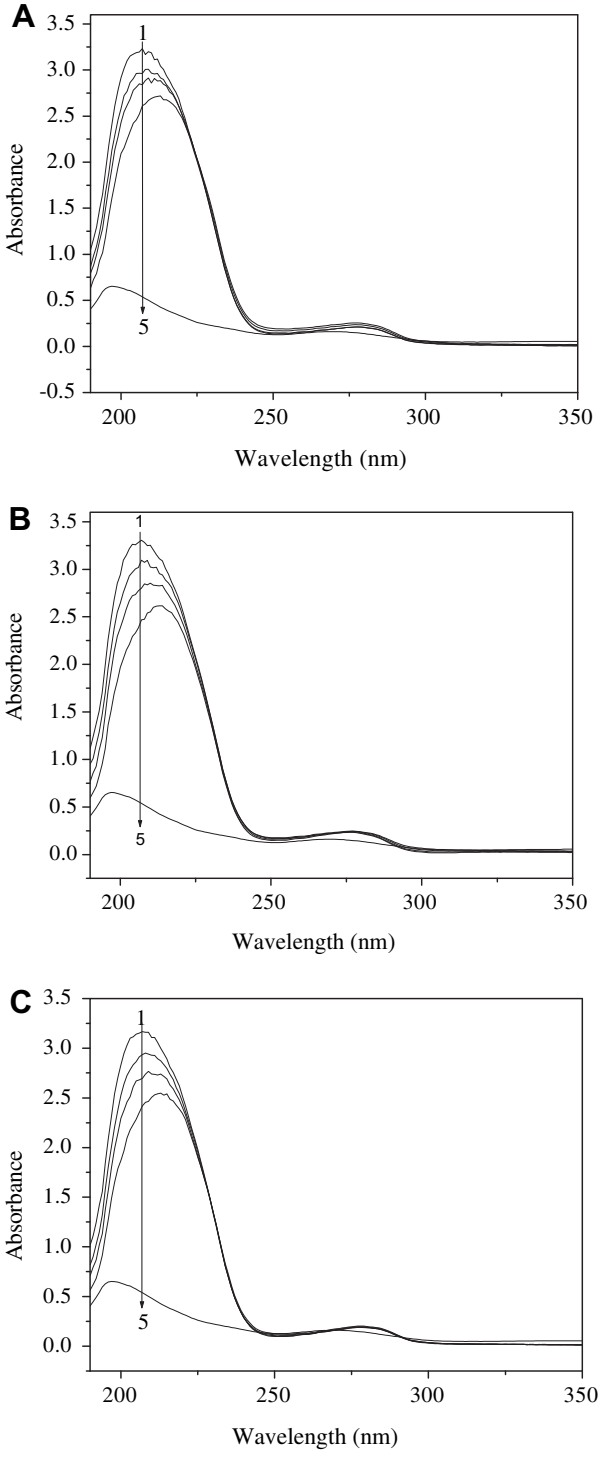

Fig. 7. UV spectra of the baicalein–BSA system without Cu^{2+} or Fe^{3+} (A) and with Cu^{2+} (B), Fe^{3+} (C): [BSA] = [Cu^{2+}] = [Fe^{3+}] = 3 μM; the concentrations of baicalein are (1–4): 0, 2, 4 and 7 μM. Curve 5: [BSA] = 0, [baicalein] = 3 μM.

baicalein–BSA system in the absence and presence of Cu^{2+} or Fe^{3+} decreased with increasing concentration of baicalein and the peak has an obvious red shift (from 208 to 213 nm). However, the absorption at 279 nm did not cause apparent change with the increase of baicalein without and with Cu^{2+} or Fe^{3+}. The literatures [35] show that the peak in the 208 nm region in the difference spectra of proteins is related to changes in the conformation of the peptide backbone associated with the helix-coil transformation [36]. In addition, the peak at 279 nm region is related to the polarity of the microenvironment around Trp and Tyr residues of BSA. The results indicate that the interaction of baicalein with BSA in the absence and presence of Cu^{2+} or Fe^{3+} may caused the conformational change of BSA, but did not change the polarity of microenvironment around Trp and Tyr residues of BSA. Furthermore, overall degree of conformational change in BSA in the presence of Cu^{2+} or Fe^{3+} is a little greater than that in the absence of Fe^{3+} on the binding of baicalein.

2.5.2. CD studies

To gain a better understanding in baicalein–protein binding mechanism and secondary structure changes of protein, additional CD measurements were performed on BSA and baicalein–BSA complex.

Fig. 8 shows the CD spectra of BSA with various amounts of baicalein in the absence and presence of Fe^{3+} at pH 7.40. They display negative CD bands in a wavelength range shorter than 240 nm. The CD spectra of BSA are characterized mainly by two negative bands at 208 nm and 222 nm. These bands are caused by a negative Cotton effect characteristic of α-helical structure [37,38]. CD is a relative powerful technique to investigate the secondary structural change of proteins, because they are, in the far ultraviolet region, related to the polypeptide backbone structure of proteins. The negative bands at 208 and 222 nm are rationalized by the $n \rightarrow \pi^*$ transition in the peptide bond of α-helical [39]. It was observed from Fig. 8 that there was an obvious reduction in both of these bands without any significant shift of the peaks in the presence of baicalein with or without Fe^{3+}, indicating the decrease of α-helical content in protein.

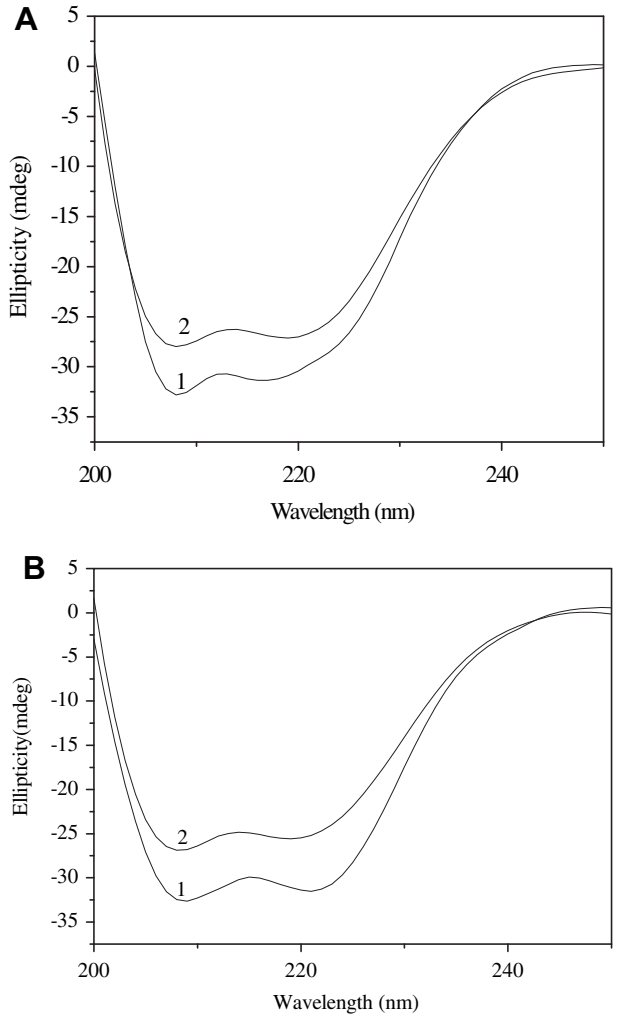

Fig. 8. CD spectra of the baicalein–BSA system without Fe^{3+} (A) and with Fe^{3+} (B). [BSA] = [Cu^{2+}] = 3 μM; baicalein to BSA ratios: (1) 0:1, (2) 2:1.

If the CD result was expressed as MRE (mean residue ellipticity) in deg cm^2 $dmol^{-1}$, the following equation would be used [40,41]:

$$\text{MRE} = \text{Observed CD(m deg)}/(10C_p nl) \quad (4)$$

where n is the number of amino acid residues (583), l is the pathlength of the cell (1 mm), and C_p is the molar concentration. The helical content was calculated from the MRE values at 208 nm using the following equation described in the previous literature [41]:

$$\alpha-\text{Helix}(\%) = [(-\text{MRE}_{208} - 4000) \times 100]/(33{,}000 - 4000) \quad (5)$$

From the above equation, the α-helix content in the secondary structure of BSA could be determined, which was presented in Table 5.

From Table 5, the content of α-helix of BSA in the presence of Fe^{3+} is nearly the same as that in the absence of Fe^{3+}, indicating that Fe^{3+} does not induce obvious conformational transition of BSA, viz. the forming of Fe^{3+}–BSA complex does not lead to the conformational transition of BSA. Therefore, the decrease of K and n in the presence of Fe^{3+} may result from the competition of the binding of Fe^{3+} and baicalein to BSA rather than the conformational changes of BSA induced by Fe^{3+}, which was in agreement with that discussed from binding distance r above. On the other hand, it is also seen from the data that the binding of baicalein with BSA with or without Fe^{3+} causes obvious conformational change, but the degree of change in conformation of BSA in the presence of Fe^{3+} is a little greater than that in the absence of Fe^{3+} on the binding of baicalein. That's to say, the effect of baicalein on the conformation of BSA with Fe^{3+} is a little more pronounced than that without Fe^{3+}. These results are in agreement with those obtained from UV–visible spectroscopy technique mentioned above.

2.5.3. Synchronous fluorescence spectroscopic studies

Synchronous fluorescence spectroscopy is a very useful method to study the microenvironment of amino acid residues by measuring the emission wavelength shift [42,43] and have several advantages, such as sensitivity, spectral simplification, spectral bandwidth reduction and avoiding different perturbing effects [44]. Vekshin [45] suggested a useful method to study the environment of amino acid residues by measuring the possible shift in wavelength emission maximum λ_{max}, the shift in position of emission maximum corresponding to the changes of the polarity around the chromophore molecule.

Table 5
The contents of α-helix in the BSA in the presence of baicalein with or without Fe^{3+}.

Experimental samples	The content of α-helix (%)
3 μM BSA	50.6
3 μM BSA + 6 μM baicalein	41.2
3 μM BSA + 3 μM Fe^{3+}	50.1
3 μM BSA + 3 μM Fe^{3+} + 6 μM baicalein	39.1

As is known, synchronous fluorescence spectra show Trp residues of BSA only at the wavelength interval ($\Delta\lambda$) of 60 nm and Tyr residues of BSA only at $\Delta\lambda$ of 15 nm. As such, Fig. 9 showed the effect of the addition of baicalein on the synchronous fluorescence spectra of Trp (1) and Tyr (2) residues in BSA without (A) or with Cu^{2+} (B), Fe^{3+}(C) when $\Delta\lambda = 60$ nm and 15 nm, respectively. It can be seen from Fig. 9 that the maximum emission wavelength of BSA in the absence and presence of Cu^{2+} or Fe^{3+} kept the position at the investigated concentrations range when $\Delta\lambda = 60$ nm and 15 nm. It implies that the interaction of baicalein with BSA does not significantly affect the polarity2 around Trp and Tyr residues microregions, which was in accordance with the result obtained from UV–visible spectroscopy technique mentioned above.

2.5.4. Three-dimensional fluorescence spectroscopic studies

Three-dimensional fluorescence spectra have become a popular fluorescence analysis technique in recent years [46]. It is well-known that three-dimensional fluorescence spectrum can provide more detailed information about the change of the configuration of proteins. In addition, the contour map can also provide a lot of important information. Figs. 10–12 presents the three-dimensional fluorescence spectra and contour ones of BSA and baicalein–BSA in the absence and presence of Cu^{2+} or Fe^{3+}, respectively. The contour map displayed a bird's eye view of the fluorescence spectra. In Figs. 10–12, peak a is the Rayleigh scattering peak and two typical fluorescence peaks (peak 1, peak 2) also could be easily observed in isometric three-dimensional projection or three-dimensional

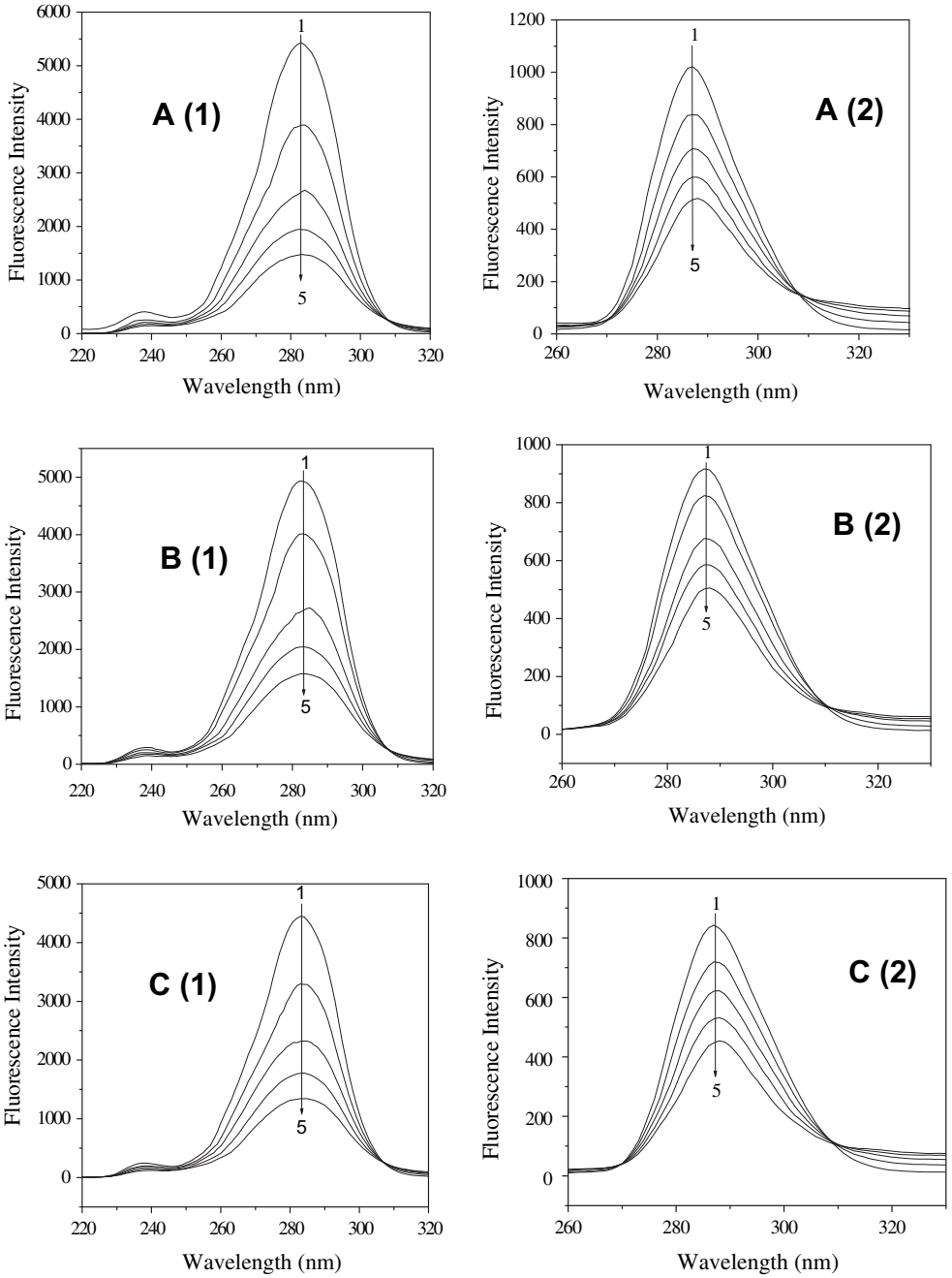

Fig. 9. Synchronous fluorescence spectra of BSA with various amounts of baicalein without Cu^{2+} or Fe^{3+} (A) and with Cu^{2+} (B), Fe^{3+} (C). (1): $\Delta\lambda = 60$ nm and (2): $\Delta\lambda = 15$ nm; [BSA] = 3 μM; [baicalein] = 0 μM (1), 1.5 μM (2), 3 μM (3), 4.5 μM (4), 6 μM (5).

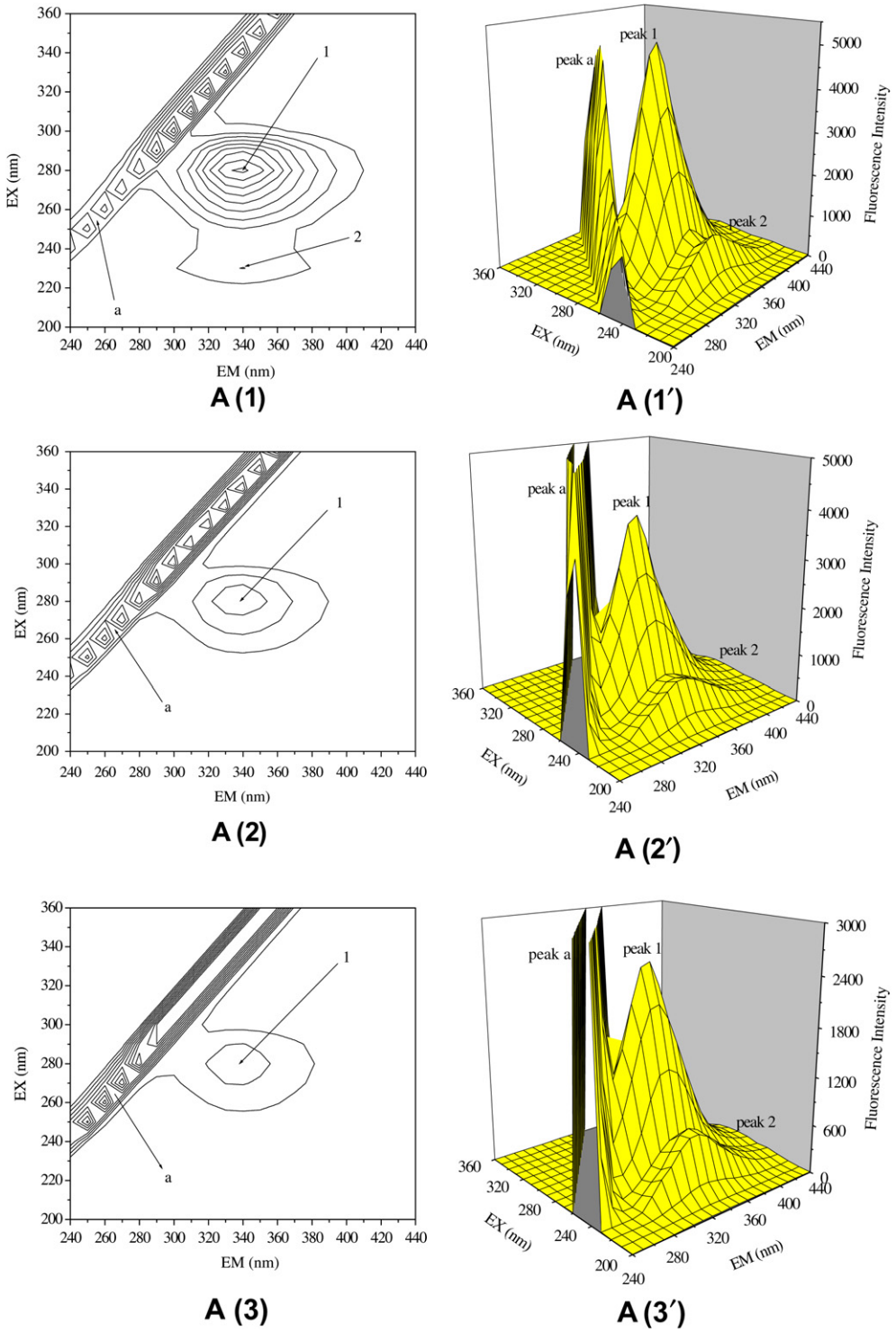

Fig. 10. The three-dimensional fluorescence projections and three-dimensional fluorescence contour map of BSA without Cu^{2+} or Fe^{3+} before (up) and after baicalein addition (down) [BSA]: A (1, 1′) 3.0 μM; A (2, 2′) 3.0 μM, A (3, 3′) 3.0 μM; [baicalein]: A (1, 1′) 0 μM, A (2, 2′) 1.5 μM, A (3, 3′) 3.0 μM.

fluorescence contour map of BSA with various amounts of baicalein in the absence and presence of Cu^{2+} or Fe^{3+}. From Figs. 10–12, it can be seen that the fluorescence intensity of peak a increased with the increase of baicalein without or with Cu^{2+} or Fe^{3+}, the possible explanation may be that a drug–BSA complex came into being after the addition of baicalein, making the diameter of BSA increased, which in turn resulted in the enhancement of the scattering effect.

As referred to peak 1, we think that it mainly reveals the spectral characteristic of tryptophan and tyrosine residues. The reason is that when serum albumin is excited at 280 nm, it mainly reveals the intrinsic fluorescence of tryptophan and tyrosine residues. Comparing with the UV–vis absorption spectra of BSA (Fig. 7, curve 1), there is an absorption peak around 279 nm and this peak is mainly caused by the transition of $\pi \rightarrow \pi^*$ of aromatic amino acids in BSA. The fluorescence intensity of the peak decreased markedly

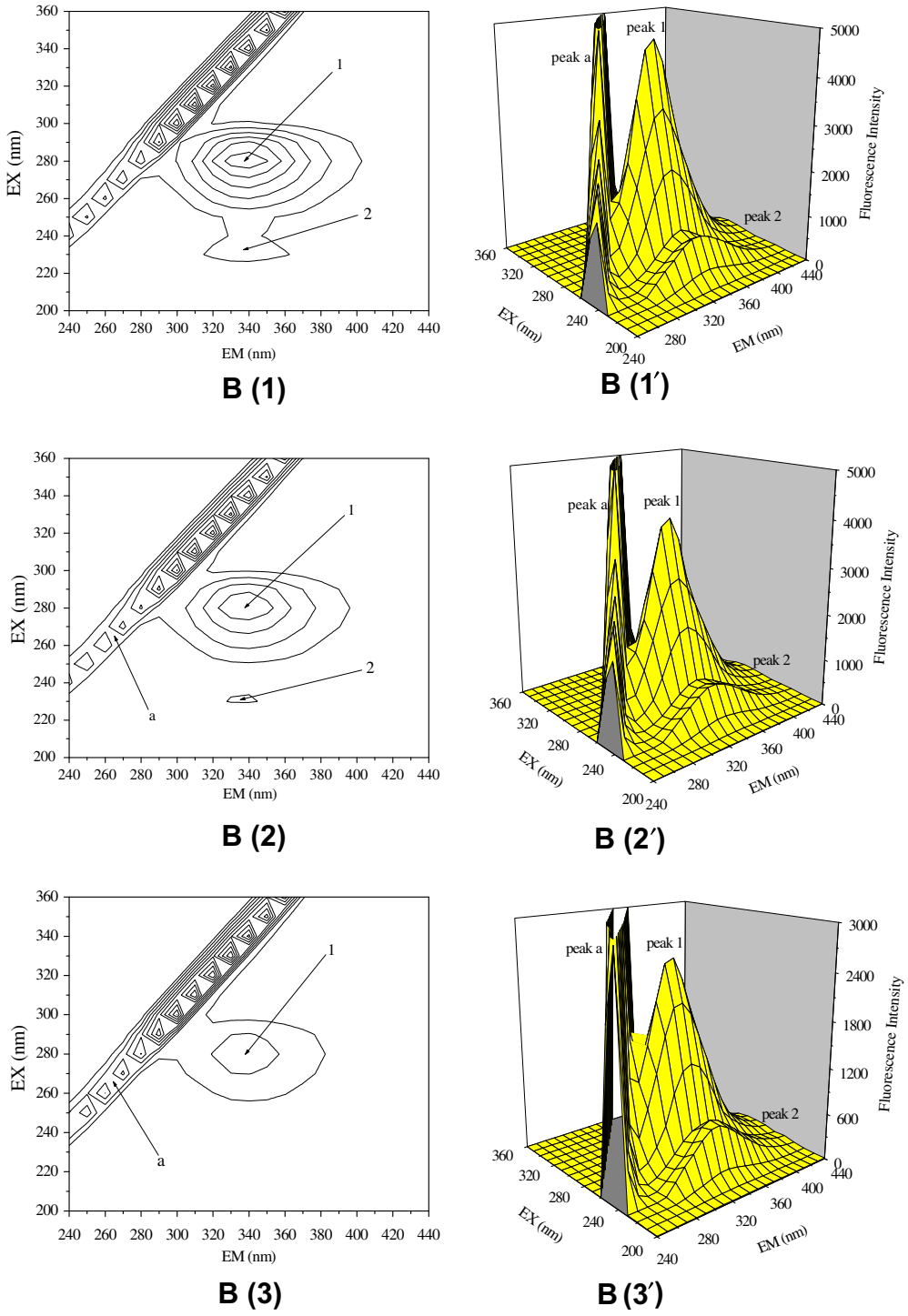

Fig. 11. The three-dimensional fluorescence projections and three-dimensional fluorescence contour map of BSA with Cu^{2+} before (up) and after baicalein addition (down) [BSA]: B (1, 1′) 3.0 μM; B (2, 2′) 3.0 μM, B (3, 3′) 3.0 μM; [baicalein]: B (1, 1′) 0 μM, B (2, 2′) 1.5 μM, B (3, 3′) 3.0 μM.

and the maximum emission wavelength of the peak was not changed following the addition of baicalein without or with Cu^{2+} or Fe^{3+} (Table 6). It implies that the addition of baicalein caused static quenching of BSA, but didn't change the polarity of this hydrophobic microenvironment (tryptophan and tyrosine residues) of BSA without or with Cu^{2+} or Fe^{3+}. This result agreed with that studied from UV–visible absorption spectroscopy and synchronous fluorescence spectra, as mentioned above. Besides peak 1, there is a new weak fluorescence peak 2. And the excitation wavelength of this peak is 230 nm, which is related to the conformation of the peptide backbone associated with the helix-coil. Comparing with the UV–vis absorbance spectra of BSA (Fig. 7, curve 1), there is a strong absorption peak around 208 nm and this peak is mainly caused by the transition of $n \rightarrow \pi^*$ of BSA's characteristic polypeptide backbone structure C=O. The emission intensity of baicalein–BSA system without or with Cu^{2+} or Fe^{3+} decreased with the

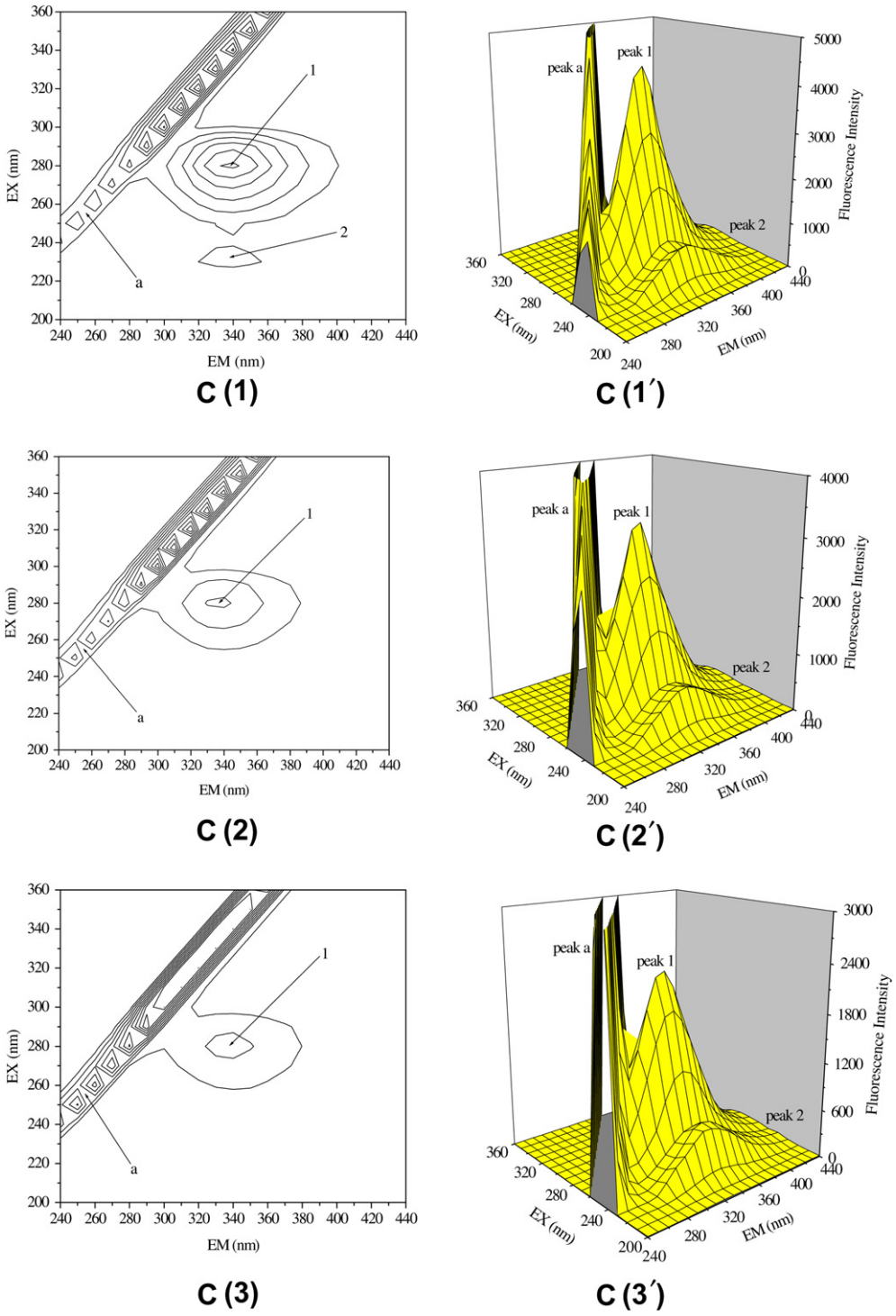

Fig. 12. The three-dimensional fluorescence projections and three-dimensional fluorescence contour map of BSA with Fe^{3+} before (up) and after baicalein addition (down) [BSA]: C (1, 1′) 3.0 μM; C (2, 2′) 3.0 μM, C (3, 3′) 3.0 μM; [baicalein]: C (1, 1′) 0 μM, C (2, 2′) 1.5 μM, C (3, 3′) 3.0 μM.

increase in baicalein concentration and the excitation peak has an obvious red shift (from 230 to 240 nm). We can conclude that the interaction of baicalein with BSA resulted in a conformational change of the protein, which was in agreement with the results obtained from UV–vis spectroscopy and CD mentioned above. In addition, obviously, the maximum absorption wavelength (208 nm) is different from the maximum excitation wavelength (230 nm). This possible reason is that part of the energy absorbed by polypeptide backbone structure C═O of BSA may be transferred to Trp and Tyr residues of BSA.

The investigation of the effect of baicalein on the conformation of BSA in the absence and presence of Cu^{2+} or Fe^{3+} is quite helpful to the understanding in biological role of serum albumin. Furthermore, our work could also be a useful guideline for further drug design.

Table 6
Three-dimensional fluorescence spectral characteristics of BSA and BSA–baicalein system.

System		Rayleigh scattering peaks	Fluorescence peak 1	Fluorescence peak 2
BSA	Peak position (EX/EM)	240/240 → 360/360	280.0/340.0	230.0/340.0
	Relative intensity, *F*	3599 → 8949	5108	1112
Baicalein/BSA (0.5:1)	Peak position (EX/EM)	240/240 → 360/360	280.0/340.0	230.0/340.0
	Relative intensity, *F*	5068 → 9231	3830	869.0
Baicalein/BSA (1:1)	Peak position (EX/EM)	240/240 → 360/360	280.0/340.0	240.0/340.0
	Relative intensity, *F*	6078 → 9232	2533	718.2
BSA/Cu^{2+} (1:1)	Peak position (EX/EM)	240/240 → 360/360	280.0/340.0	230.0/340.0
	Relative intensity, *F*	1757 → 4625	4733	925.3
Baicalein/BSA/Cu^{2+} (0.5:1:1)	Peak position (EX/EM)	240/240 → 360/360	280.0/340.0	230.0/340.0
	Relative intensity, *F*	1859 → 4657	3977	833.3
Baicalein/BSA/Cu^{2+} (1:1:1)	Peak position (EX/EM)	240/240 → 360/360	280.0/340.0	240.0/340.0
	Relative intensity, F	2945 → 6831	2547	679.5
BSA/Fe^{3+} (1:1)	Peak position (EX/EM)	240/240 → 360/360	280.0/340.0	230.0/340.0
	Relative intensity, *F*	1519 → 4382	4360	865.5
Baicalein/BSA/Fe^{3+} (0.5:1:1)	Peak position (EX/EM)	240/240 → 360/360	280.0/340.0	230.0/340.0
	Relative intensity, *F*	2627 → 7395	3203	717.4
Baicalein/BSA/Fe^{3+} (1:1:1)	Peak position (EX/EM)	240/240 → 360/360	280.0/340.0	240.0/340.0
	Relative intensity, *F*	3548 → 9121	2279	605.8

3. Conclusion

In the paper, the binding properties of baicalein to BSA were characterized by measuring the fluorescence, UV–vis spectroscopy, CD, and the three-dimensional (3D) spectra. The fluorescence quenching mechanism and binding mode were investigated at pH 7.40. In our experiment, the presence of Cu^{2+} and Fe^{3+} ions decreased the binding constants of baicalein–BSA complex, which may arise from the competition of baicalein and metal ions binding to BSA. UV–vis spectroscopy, CD and three-dimensional (3D) fluorescence spectra show conformational change upon addition of baicalein without or with Cu^{2+} or Fe^{3+}at pH 7.40.

The binding study of drugs to proteins is greatly important in pharmacy, pharmacology and biochemistry and so on. This study can provide important insight into the interactions of the physiologically important BSA with drugs. Besides, useful information can be also obtained about the effect of environment on the structure features of BSA which may be correlated to its physiologically activity.

4. Experimental

4.1. Materials

BSA was purchased from Sigma (USA). Baicalein was of analytical grade and purchased from the National Institute for Control of Pharmaceutical and Bioproducts, China. All other reagents were of analytical grade. Double-distilled water was used throughout experiments. Solutions of BSA were prepared in 20 mM phosphate buffered saline (PBS) at pH 7.4, whose ion strengths were kept at 0.1 M. A 0.5 mM water solution of baicalein was used for all binding experiments.

4.2. Equipments and spectral measurements

Fluorescence measurements were performed on an FL-4500 spectrofluorophotometer (Japan). UV absorption spectra were measured on a UV-3010 UV–vis spectrophotometer in a 1-cm cuvette. Circular dichroism (CD) spectra were recorded on an Olis DSM-1000 automatic recording spectropolarimeter (USA) over the range of 200–250 nm at an interval of 0.5 nm in a 1-mm cell equipped with a temperature controlling unit.

4.3. Procedures

A 3 mL solution, containing appropriate concentration of BSA, was titrated by successive additions of a 0.5 mM solution of baicalein. Titrations were done manually by using trace spyinges.

The fluorescence emission spectra were then measured at 310 K and were recorded in a wavelength range of 290–500 nm following an excitation at 295 nm, the excitation and emission bandwidths were 5 nm. The quenching effect of ethanol and the effect of ethanol on BSA conformation have been investigated, and the result indicated that the effect of ethanol on the interaction of baicalein with BSA could be negligible in the amount used in our experiment.

UV absorption spectra were measured from 190 nm to 350 nm on a UV-3010 UV–vis spectrophotometer equipped a 1-cm cuvette.

CD spectra were recorded over a wavelength range of 200–250 nm with a scan of 50 points at 310K in a thermostated cell holder, with three scans averaged for each CD spectra. Results are expressed as ellipticity (mdeg), which was obtained in mdeg directly from the instrument.

Synchronous fluorescence spectra were obtained by scanning simultaneously the excitation and emission monochromator. The wavelength interval ($\Delta\lambda$) is fixed individually at 15 and 60 nm, at which the spectrum only shows the spectroscopic behavior of Tyr and Trp residues of BSA, respectively.

The three-dimensional fluorescence spectrums were performed under the following conditions: the emission wavelength scan range was recorded between 240 nm and 440 nm, the excitation wavelength scan range was recorded from 200 to 360 nm at 10 nm increments. The number of scanning curves was 17, and other scanning parameters were just the same as the fluorescence quenching spectra.

Acknowledgements

We are grateful to the National Natural Science Foundation of China (no. 20902043) and the Natural Science Foundation of Henan Province, China (no. 102300410220) for financial support of this work.

References

[1] P.B. Kandagal, S. Ashoka, J. Seetharamappa, S.M.T. Shaikh, Y. Jadegoud, O.B. Ijare, Study of the interaction of an anticancer drug with human and

bovine serum albumin: spectroscopic approach, J. Pharm. Biomed. Anal. 41 (2006) 393–399.
[2] X. Zhu, J. Sun, Y. Hu, Determination of protein by hydroxypropyl-β-cyclodextrin sensitized fluorescence quenching method with erythrosine sodium as a fluorescence probe, Anal. Chim. Acta 596 (2007) 298–302.
[3] Y.Q. Wang, H.M. Zhang, G.C. Zhang, Studies of the interaction between palmatine hydrochloride and human serum albumin by fluorescence quenching method, J. Pharm. Biomed. Anal. 41 (2006) 1041–1046.
[4] I. Petitpas, T. Grune, A.A. Bhattacharya, S. Curry, Crystal structures of human serum albumin complexed with monounsaturated and polyunsaturated fatty acids, J. Mol. Biol. 314 (2001) 955–960.
[5] M. Dockal, D.C. Carter, F. Ruker, Conformational transitions of the three recombinant domains of human serum albumin depending on pH, J. Biol. Chem. 275 (2000) 3042–3050.
[6] B. Ahmad, Ankita, R.H. Khan, Urea induced unfolding of F isomer of human serum albumin: a case study using multiple probes, Arch. Biochem. Biophys. 437 (2005) 159–167.
[7] X.M. He, D.C. Carter, Atomic structure and chemistry of human serum albumin, Nature 358 (1992) 209–215.
[8] T. Peters, All about Albumin: Biochemistry, Genetics and Medical Application. Academic Press, Inc., New York, 1996.
[9] Y.Q. Wang, H.M. Zhang, G.C. Zhang, W.H. Tao, Z.H. Fei, Z.T. Liu, Spectroscopic studies on the interaction between silicotungstic acid and bovine serum albumin, J. Pharm. Biomed. Anal. 43 (2007) 1869–1875.
[10] N. Zhou, Y.Z. Liang, P. Wang, 18β-Glycyrrhetinic acid interaction with bovine serum albumin, J. Photochem. Photobiol., A 185 (2007) 271–276.
[11] C. Bertucci, S. Cimitan, A. Riva, P. Morazzoni, Binding studies of taxanes to human serum albumin by bioaffinity chromatography and circular dichroism, J. Pharm. Biomed. Anal. 42 (2006) 81–87.
[12] Y.J. Hu, Y. Liu, R.M. Zhao, J.X. Dong, S.S. Qu, Spectroscopic studies on the interaction between methylene blue and bovine serum albumin, J. Photochem. Photobiol., A 179 (2006) 324–329.
[13] Y.P. Wang, Y.L. Wei, C. Dong, Study on the interaction of 3,3-bis (4-hydroxy-1-naphthyl)-phthalide with bovine serum albumin by fluorescence spectroscopy, J. Photochem. Photobiol., A 177 (2006) 6–11.
[14] V. Anbazhagan, R. Renganathan, Study on the binding of 2,3-diazabicyclo [2.2.2]oct-2-ene with bovine serum albumin by fluorescence spectroscopy, J. Lumin. 128 (2008) 1454–1458.
[15] C.C. Lin, D.E. Shieh, The anti-inflammatory activity of *Scutellaria rivularis* extracts and its active components, baicalin, baicalein and wogonin, J. Am. Chin. Med. 24 (1996) 31–36.
[16] L. Wang, Y. Ling, Y. Chen, C.L. Li, F. Feng, Q.D. You, N. Lu, Q.L. Guo, Flavonoid baicalein suppresses adhesion, migration and invasion of MDA-MB-231 human breast cancer cells, Cancer Lett. 297 (2010) 42–48.
[17] C.Q. Jiang, M.X. Gao, X.Z. Meng, Study of the interaction between daunorubicin and human serum albumin, and the determination of daunorubicin in blood serum samples, Spectrochim. Acta, Part A 59 (2003) 1605–1610.
[18] M. Guo, W.J. Lu, M.H. Li, W. Wang, Study on the binding interaction between carnitine optical isomer and bovine serum albumin, Eur. J. Med. Chem. 43 (2008) 2140–2148.
[19] T.G. Dewey (Ed.), Biophysical and Biochemical Aspects of Fluorescence Spectroscopy, Plenum Press, New York, 1991, pp. 1–41.
[20] M.X. Xie, M. Long, Y. Liu, C. Qin, Y.D. Wang, Characterization of the interaction between human serum albumin and morin, Biochim. Biophys. Acta 1760 (2006) 1184–1191.
[21] D.J. Li, J.F. Zhu, J. Jin, Spectrophotometric studies on the interaction between nevadensin and lysozyme, J. Photochem. Photobiol., A 189 (2007) 114–120.
[22] D.J. Li, B.M. Ji, J. Jin, Spectrophotometric studies on the binding of Vitamin C to lysozyme and bovine liver catalase, J. Lumin. 128 (2008) 1399–1406.
[23] W.R. Ware, Oxygen quenching of fluorescence in solution: an experimental study of the diffusion process, J. Phys. Chem. 66 (1962) 455–458.
[24] M.X. Xie, X.Y. Xu, Y.D. Wang, Interaction between hesperetin and human serum albumin revealed by spectroscopic methods, Biochim. Biophys. Acta 1724 (2005) 215–224.
[25] U. Kragh-Hansen, Molecular aspect of ligand binding to serum albumin, Pharmacol. Rev. 33 (1981) 17–53.
[26] P. Wu, L. Brand, Resonance energy transfer: methods and applications, Anal. Biochem. 218 (1994) 1–13.
[27] Y.J. Hu, Y. Liu, J.B. Wang, X.H. Xiao, S.S. Qu, Study of the interaction between monoammonium glycyrrhizinate and bovine serum albumin, J. Pharm. Biomed. Anal. 36 (2004) 915–919.
[28] L. Cyril, J.K. Earl, W.M. Sperry, Biochemists Handbook. E & FN Epon Led. Press, London, 1961, p. 83.
[29] C.Q. Jiang, T. Wang, Study of the interactions between tetracycline analogues and lysozyme, Bioorg. Med. Chem. 12 (2004) 2043–2047.
[30] B. Valeur, J.C. Brochon, New Trends in Fluorescence Spectroscopy, sixth ed. Springer Press, Berlin, 1999.
[31] J.N. Tian, J. Liu, Z.D. Hu, X.G. Chen, Interaction of wogonin with bovine serum albumin, Bioorg. Med. Chem. 13 (2005) 4124–4129.
[32] M.H. Rahman, T. Maruyama, T. Okada, K. Yamasaki, M. Otagiri, Study of interaction of carprofen and its enantiomers with human serum albumin—I: mechanism of binding studied by dialysis and spectroscopic methods, Biochem. Pharmacol. 46 (1993) 1721–1731.
[33] P.D. Ross, S. Subramanian, Thermodynamics of protein association reactions: forces contributing to stability, Biochemistry 20 (1981) 3096–3102.
[34] S.Y. Bi, D.Q. Song, Y. Tian, X. Zhou, X. Liu, H.Q. Zhang, Spectroscopic characterization of effective components anthraquinones in Chinese medicinal herbs binding with serum albumins, Spectrochim. Acta, Part A 61 (2005) 629–636.
[35] A.N. Glazer, E.L. Smith, Studies on the ultraviolet difference spectra of proteins and polypeptides, J. Biol. Chem. 236 (1961) 2942–2947.
[36] H. Polet, J. Steinhardt, Binding-induced alterations in ultraviolet absorption of native serum albumin, Biochemistry 7 (1968) 1348–1356.
[37] N. Greenfield, G.D. Fasman, Computed circular dichroism spectra for the evaluation of protein conformation, Biochemistry 8 (1969) 4108–4116.
[38] I. Staprans, S. Watanabe, Optical properties of troponin, tropomyosin, and relaxing protein of rabbit skeletal muscle, J. Biol. Chem. 245 (1970) 5962–5966.
[39] P. Yang, F. Gao, The Principle of Bioinorganic Chemistry. Science Press, 2002, p. 349.
[40] Y.H. Chen, J.T. Yang, H.M. Martinez, Determination of the secondary structures of proteins by circular dichroism and optical rotatory dispersion, Biochemistry 11 (1972) 4120–4131.
[41] H. Gao, L. Lei, J. Liu, Q. Kong, X. Chen, Z. Hu, The study on the interaction between human serum albumin and a new reagent with antitumour activity by spectrophotometric methods, J. Photochem. Photobiol. A 167 (2004) 213–221.
[42] G.Z. Chen, X.Z. Huang, Z.Z. Zheng, J.G. Xu, Z.B. Wang, Fluorescence Analytical Method, second ed. Science Press, Beijing, 1990, p. 117.
[43] W.C. Abert, W.M. Gregory, G.S. Allan, The binding interaction of Coomassie blue with proteins, Anal. Biochem. 213 (1993) 407–413.
[44] S. Ashoka, J. Seetharamappa, P.B. Kandagal, S.M.T. Shaikh, Investigation of the interaction between trazodone hydrochloride and bovine serum albumin, J. Lumin. 121 (2006) 179–186.
[45] N.L. Vekshin, Separation of the tyrosine and tryptophan components of fluorescence using synchronous scanning method, Biofizika 41 (1996) 1176–1182.
[46] G. Weber, Enumeration of components in complex systems by fluorescence spectrophotometry, Nature 190 (1961) 27–34.